JOINT INSTITUTE FOR NUCLEAR RESEARCH
Frank Laboratory of Neutron Physics

FINAL REPORT ON THE START PROGRAMME

Obtaining and studying structures of the "quantum" diode type based on hydrated ZrO_2 nanopowders for alternative energy and nanoelectronics

Supervisor:

Dr. Aleksandr Doroshkevich

Student:

Jeannine Milanés, Mexico
Western Institute of Technology and Higher Education

Participation period:
July 06 – August 16,
Summer Session 2025

Dubna, 2025

Contents

Abstract

This research project investigates the electrical behavior of planar heterojunctions formed by ZrO_2-8% Y_2O_3 nanoparticle thin films under controlled hydration and deuteration at 65%, 75%, and 85% humidities. Reference, non-variable contacts were prepared with 10 nm particles annealed at 500 °C, while opposing, variable contacts contained larger particles (12–16 nm) obtained at 600-800 °C. Current–voltage measurements over ±2 V showed mainly linear responses for contacts of identical or similar particle size, with weak rectifying behavior emerging mainly in 500-700 °C pairs at higher humidity. Deuterated samples showed higher currents than hydrated contacts, suggesting isotope dependent enhancement of surface ionic conduction. Distinct valleys in certain samples were attributed to dissociation processes. The limited voltage range, thin film non-uniformities, and polarization effects likely caused the exhibited weaker rectification; extending the sweep range and refining deposition methods may give way to rectifying contact-like properties in the nanopowder based planar heterojunctions.

1. Introduction

Modern electronic devices rely on conventional semiconductor junctions, which tend to be inefficient and unstable, leading to energy losses, performance degradation, and limited sustainability. These limitations are mostly due to diffusion-induced degradation, because of doped junction's inherent instability. In traditional electronics, charge carriers are primarily introduced by chemical doping. When paired with different semiconductors, heterojunctions are formed, enabling functionality by bandgap engineering. However, these interfaces are prone to scatter charge carriers, ion migration, defect formation, and thermomechanical stress, resulting in device failure and electronic waste [1]. Additionally, many advanced semiconductors, which aim to increase efficiency, tend to use toxic and rare elements, such as gallium and indium [2]. This is particularly problematic for green technologies, where efficiency, material sustainability, and long-term usage are most relevant.

Previous research has emphasized the need for innovative materials and processes that improve traditional electronic systems and overcome the limitations present in conventional electronics. Despite these efforts, no other system that can meet the characteristics and provide similar or better results has been developed or implemented [2], [3].

In this report, an exploration into hydrated ZrO_2 nanopowder is proposed as a foundation to develop "quantum" diodes that use diverse nanoscale effects to create stable and efficient devices. These innovations could lead to revolutionary alternative energy systems and nanoelectronics that can reduce waste, improve charge transport, and use conversion mechanisms that do not require toxic or rare materials.

1.1 Physical Principles

1.1.1 Fractal Geometry and One-Dimensional Modeling

One of the most representative ways to approach fractal geometry is through the construction of a Koch curve; Koch's fractal theory describes a geometric curve that is built form an iterative process using an equilateral triangle as basis, eventually evolving into a snowflake-like structure with an infinite length that contains a finite area that remains similar to the initial geometry (**Figure *1.*** Evolutive Koch curve for fractal formation [6].Figure 1) [4]. This recursive growth introduces features to the system's architecture, such as roughness and irregularity, which result in a variety of scale dependent properties, participating in surface interactions, diffusion dynamics, and local field enhancements in nanostructures [5].

Additionally, the probability of fractal formation considers parameters related to thermal fluctuations: at higher temperatures, the system is more capable of forming stable high order configurations, and vice versa. Therefore, measured physical properties must be an average over certain segments in order to gather data that reflects the evolution of the system.

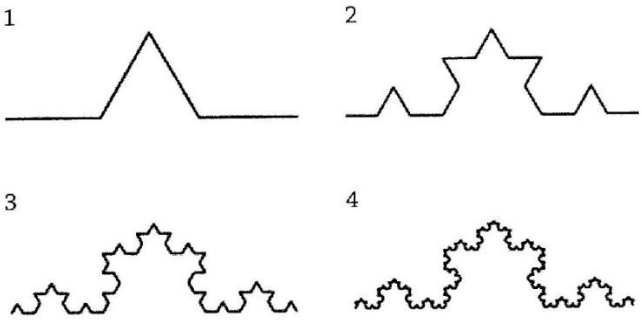

Figure 1. Evolutive Koch curve for fractal formation [6].

1.1.2 Near-Surface Electronic Structure in Ionic Crystals

In ionic crystals, surface ions have fewer neighbors than in bulk, resulting in a reduced Madelung constant and shallower electrostatic potential well, shifting surface localized states toward the inside of the band gap. When the surface additionally has curvature, such as convexity, ions have even fewer neighbors (than flat surfaces), allowing the appearance of a graded band gap across the curved surface. As this curvature increases, the density and spatial extent of Tamm surface states also grows, resulting in their delocalization, which boosts their reactivity and creates new electronic pathways [7].

1.1.3 Surface States, Curvature, Fractal Modulation

The Tamm model describes surface localized electronic states at crystal and vacuum interfaces whose wave functions decay exponentially into the vacuum because of abrupt periodic potential termination [8]. In ionic nanoparticles, quantum confinement and increasing surface curvature work together to elevate these Tamm levels toward the conduction band edge, making them more chemically active; the decay length increases, extending the orbital into the surrounding medium [8], [9]. The Madelung energy per ion, reflecting electrostatic binding, decreases at surfaces and declines further with positive curvature (convex regions), due to reduced coordination. In a fractal surface made up of convex and concave features, these effects produce a graded band gap which is narrower at peaks with wider in indentations [9]. Previous works have demonstrated that Tamm levels on convex spherical regions shift toward the middle of the band gap as curvature increases, leading to enhanced accessibility and reactivity of these surface states [9].

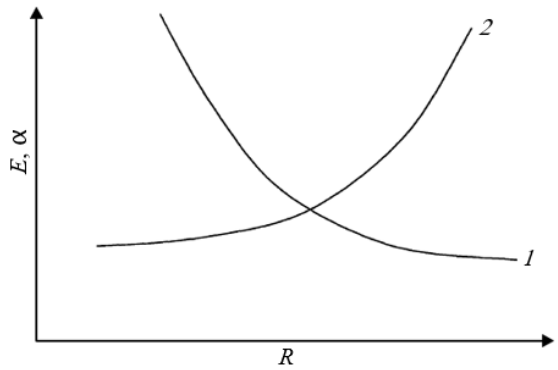

Figure 2. Dependence of the energy of Tamm's level and damping of the wave function of a Tamm electron on the nanoparticle radius [10].

Integrating quantum confinement, curvature dependent Madelung shifts, and fractal modulation results in extended Tamm orbitals that are more chemically accessible and reactive. This enhances heterogeneous catalytic activity and can boost optical effects like exciton generation in quantum dots, where coupled surface and bulk states optimize energy transfer pathways [7].

1.1.4 Surface Localized Electronic States Beyond Tamm States

Apart from the previously reviewed Tamm surface states, other localized electronic levels appear depending on the kind of interaction between electron energy and surface potential structure. Wave functions can split according to three different regimes: states within the forbidden gap, states that have a graded band gap region, which reflect spatial variation in potential near curved surfaces, and states within a "wedged" potential well at sharp edges. In this last case, electrons occupy discrete levels described by Airy function-like wave functions [9].

These localized states occupy an energy region between Tamm levels and bulk energy bands, working as intermediate steps that aid with charge transfer across interfaces. They are not purely bound to the surface or delocalized; said systems represent spatially confined yet energetically different states because of their geometrical differences.

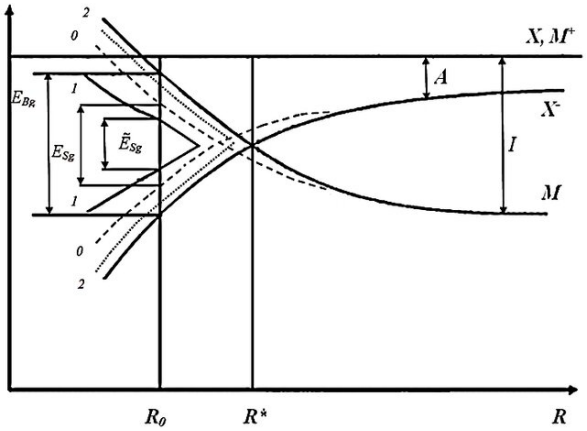

Figure 3. Madelung-Seitz diagram illustrating bulk and surface electron level positions [11].

1.1.5 Contact Potential Difference in Nanoparticle Assemblies

When two identically sized nanoparticles of the same radius are brought into contact, bulk Fermi levels should align, resulting in zero net voltage. However, quantum order fluctuations are able to break symmetry due to polarization. This happens when the spontaneous transfer of one (or more) electron from one particle to another acts like an autocatalytic cascade, polarizing the environment and creating a small yet stable contact voltage [7].

In the case of systems of nanoparticles with different radii, quantum confinement has a more notorious effect. As particle size decreases, the band gap widens, and deep level donor energies shift depending on curvature and dielectric environment, while larger particles have smaller shifts. This size-dependent shift results in a Fermi level mismatch between otherwise identical nanoparticles. When they come in contact, electrons flow until the Fermi levels align, resulting in a stable contact potential difference, similar to rectifying contact behavior in bulk systems [7].

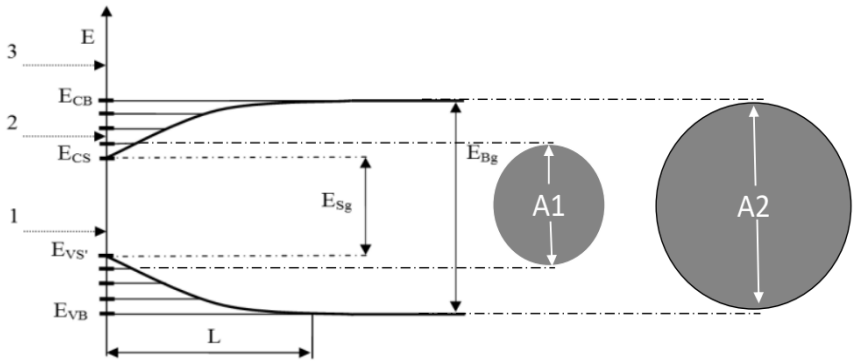

Figure 4. Size dependent band gap widening due to electron confinement.

Spontaneous polarization at identical nanoparticles and size-driven level shifts at different sizes lead to observable voltages across nanoparticle interfaces, governing rectifying behavior in nanoscale assemblies without the use of traditional heterojunctions.

1.2 Project goals

The project aims to study the time dependence of the electrical properties of a rectifying contact based on hydrated and deuterated 10, 12, 14, and 16 nm yttrium-stabilized zirconia (YSZ).

2. Methodology

2.1 Material synthesis and solution preparation

Multiple solutions of ZrO_2–8% Y_2O_3 nanopowder were synthesized using annealed zirconium (Zr) pigment powder as the precursor material. The nanopowder was dispersed in an aqueous polyvinyl alcohol (PVA) solution at a fixed ratio of 1:10 to ensure stability, where PVA prevents particle agglomeration while promoting uniform deposition.

2.1.1 Fabrication of test samples and environmental control

Two gold-plated contact pads with their respective YSZ nanopowder solutions were fabricated for each set of samples by drop casting the prepared solutions. To investigate the influence of particle size on electrical and environmental performance, a comparative approach for nanoparticle sizes was used. The reference contact pad was consistently prepared using a 10 nm YSZ nanopowder solution, thermally treated at 500°C. Variable contact pads were fabricated using nanopowder solutions with average particle sizes of 12, 14, and 16 nm, corresponding to annealing temperatures of 600°C, 700°C, and 800°C, respectively.

Figure 5. 500 (left) single drop deposition and 800 (right) linear drop deposition over gold-plated contact pad.

After deposition, the sample to be analyzed was placed in a sealed container under controlled humidity conditions of 65%, 75%, and 85%, which were conserved using saturated salt solutions of potassium chloride (KCl), sodium chloride (NaCl), and sodium bromide (NaBr), respectively. Water (H_2O) and deuterium oxide (D_2O) environments were used to examine the system's response to variation in moisture content.

2.1.2 Electrochemical characterization

Each contact pad was connected to 0.01 mm diameter copper wires via soldering, and the connections were then connected to an impedance meter to proceed with electrochemical characterization. Current–voltage (V–I) measurements were obtained by performing consecutive linear sweep cycles for each sample at the three specified humidity levels. This procedure allowed for the systematic evaluation of voltamperic behavior as a function of both particle size and environmental moisture, as well as its time dependency.

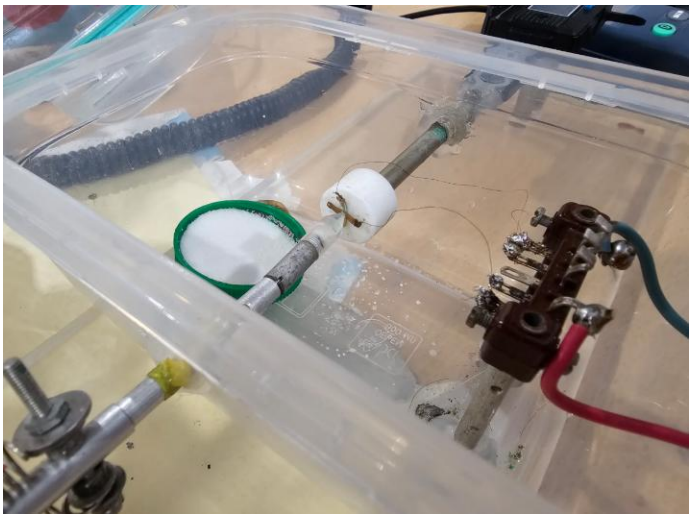

Figure 6. Experimental setup of container with humidity-retaining salt, placed and connected contacts, and wires connecting to anode and cathode.

2.2 Thin film fabrication

Various thin film fabrication techniques were used to optimize the fabrication process and analyze the influence of different preparation methods, sample composition, and geometries on electrochemical measurements. Prior to deposition, all gold contact pads were thoroughly cleaned using ethanol to remove surface contaminants and guarantee adhesion.

For thin films prepared with drop casting deposition, solution handling was achieved using syringe needles to deposit approximate volumes of the suspensions. The reference contact (500°C) received a single droplet deposited at the center of the contact pad and allowed to dry in room temperature conditions. The variable contacts (600°C, 700°C, and 800°C) were fabricated using the same technique, yet the initial droplet was “dragged” across the contact surface using the syringe needle, creating a linear segment of approximately 0.5 cm in length that covered the contact width (as shown in Figure 5). This process was repeated for all contacts after completely drying the initial film, resulting in a total of two deposited droplets.

Thin films were also fabricated via spray pyrolysis, in which YSZ colloidal solutions were diluted in distilled water at a 1:10 ratio to ensure atomization. Using an aerograph system, the diluted suspensions were sprayed directly onto the gold contact pads, which were maintained at a constant temperature of approximately 240°C on a magnetic heating plate to facilitate drying and film formation. The nozzle to substrate distance was kept at around 20 cm, and approximately 20 spray passes were performed per sample to ensure uniform coverage. This deposition process was only used for 500-500 and 500-600, with the purpose of further studying and comparing its effects in morphology and thin film formation in the future.

3. Results

Current-voltage behavior and estimated parameters for chemically identical samples (ZrO_2–8% Y_2O_3) with a contact fabricated at 500 °C and its counterpart fabricated at 800 °C are shown in Figure 7 and Table 1; these curves were obtained at 85% relative humidities of both H_2O and D_2O. Values for the H2O 500-800 I-V curve remain undefined due to it presenting clear linear behavior.

Table 1. Estimated limiting parameters of heterojunctions on varying moisture sources for differently sized contacting nanoparticles (500-800).

Sample	Maximum reverse voltage (V)	Peak reverse current (μA)	Maximum forward voltage (V)	Peak forward current (μA)
H_2O 500-800 (H885Y5_8_LIN-2V)	-	-	-	-
D_2O 500-800 (D885Y5_8_LIN-2V)	1.03	18.02	-1.84	-28.59

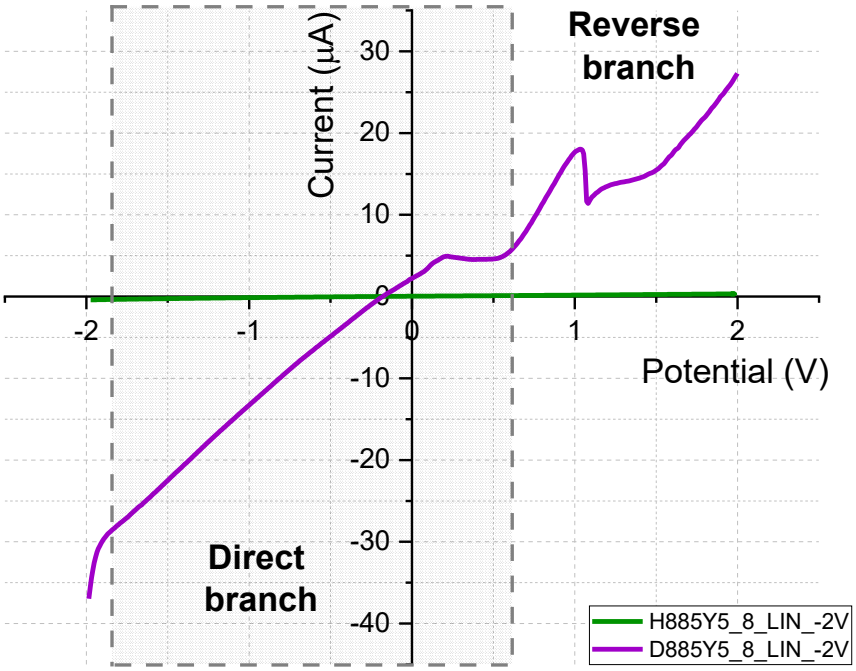

Figure 7. I-V dependences and estimated parameters of different sized nanoparticles under high relative (85%) hydration and deuteration conditions.

I-V curves were obtained for systems with a fixed contact at 500 °C and variable opposing contacts prepared at 500, 600, 700, and 800 °C. Measurements were carried out at a range of ±2V under 65%, 75%, and 85% humidity conditions, with both hydration and deuteration tested. Across all curves, contacts of the same or similar particle size, such as 500-500 and 500-600, display essentially linear behavior, characteristic of Ohmic contacts. In contrast, samples with a larger size

difference exhibit diode-like behavior, characterized by high forward currents in one bias direction and suppressed current in the opposite direction.

Figure 8a **Figure *8.*** I-V family of curves under hydration conditions at (a) 65%, (b) 75%, and (c) 85% humidity.shows the I–V characteristics of same and different size contact sets after exposure to low humidity (65 %) under hydration conditions. Under these conditions, most contacts exhibit linear responses with relatively low current magnitudes; the highest currents measured remain below 6 µA. A noticeable curvature is observed for the 500-700 contact, which can be attributed to the size gradient between the nanoparticle populations in contact.

At 75% Figure 8b relative humidity, the 500-500, 500-600, and 500-700 contacts still present largely linear I–V responses, although current values begin to deviate more clearly from zero. For the 500-700 sample, the influence of the size gradient remains evident, but the curve is nearly symmetrical, indicating that rectification is not yet fully established. In comparison, at the higher humidity level of 85% Figure 8c, the 500-700 contact begins to display rectifying contact characteristics, with a steeper forward branch and reduced reverse current, while the remaining samples continue to show linear behavior with low current variation. It is also noted that the maximum current for the 500-700 contact at this humidity increases to 18.6 µA. In some cases, the I-V curves present a horizontal shift form the origin, indicating a voltage offset. This behavior can be attributed to polarization effects at the contact or electrode interfaces, where slow-moving ionic charges accumulate and create an internal bias that alters the apparent zero-voltage condition [7].

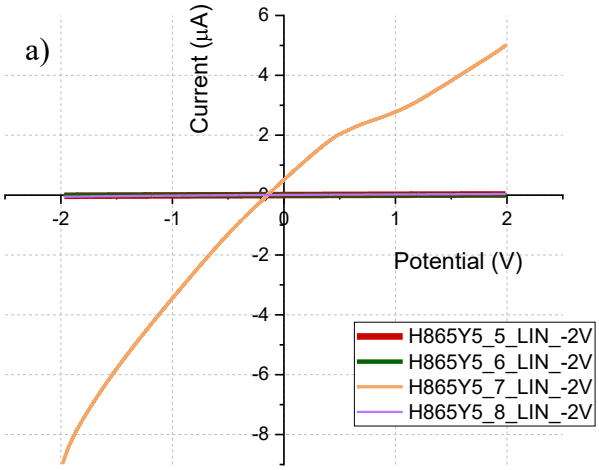

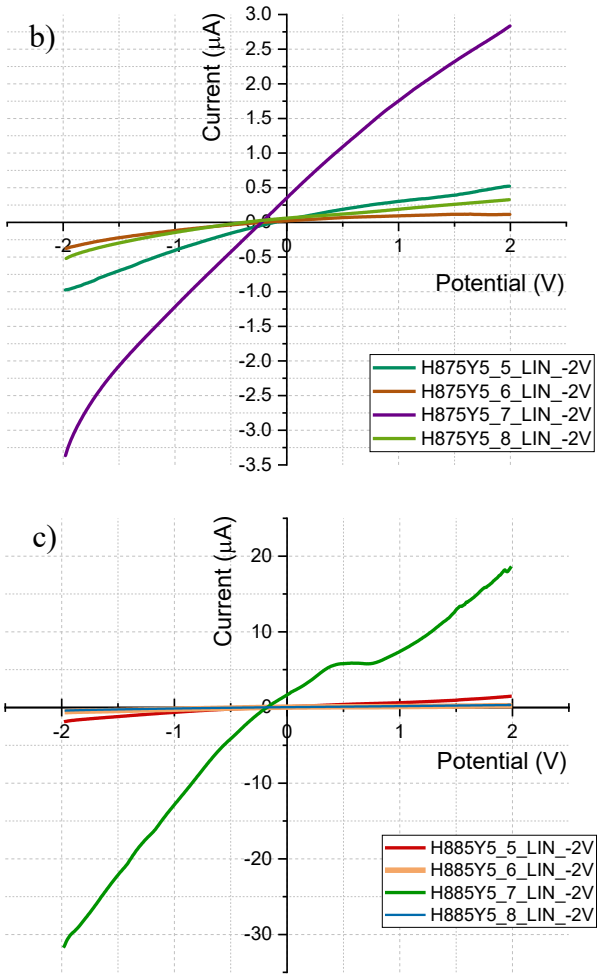

Figure 8. I-V family of curves under hydration conditions at (a) 65%, (b) 75%, and (c) 85% humidity.

The I-V characteristics of the samples after deuteration Figure 9 exhibit similar behaviors to those observed for the hydrated samples. Across all curves, contacts with the same or small size difference, such as 500-500 and 500-600, show predominantly linear behavior characteristic of Ohmic contacts, with low currents. In contrast, contacts with larger size disparities, particularly 500-700 and 500-800, tend to exhibit noticeable curvature in their I–V profiles, which can be attributed to Fermi-level differences created by the size gradient [7].

At low humidity deuteration (65%, Figure 9a), same and similar size contacts have low currents and linear responses, though 500-700 and 500-800 already display distinguishable curvature in the forward branch. At medium humidity (75%, Figure 9b), currents increase across all contacts, and the pairs 500-700 and 500-800 develop more pronounced asymmetry. Notoriously, the current values under deuteration at this humidity are higher than those found for the hydrated samples, suggesting that the composition of the moisture source influences the conductivity of the surface hydration shell [7]. At high humidity deuteration (85%, Figure 9c), 500-700 shows further increase in forward current and retains curvature, yet doesn't appear to display clear rectifying contact

characteristics, while 500-800, even after showing curvature at intermediate humidity, reverts to a more linear, Ohmic-like response with slightly noticeable rectifying characteristics.

Similarly to Figure 8, a horizontal offset relative to the origin can also be observed; this shift can also be attributed to polarization effects at the contact interface, which happens due to possible ionic accumulation that generates internal bias and displaces the potential [7].

In Figure 9c, distinct valleys appear between approximately +1 and +2 V in curves for deuterated 500-700 and 500-800 contacts. These valleys are attributed to dissociation processes occurring within the surface hydration (or deuteration) layer. Additionally, there appears to be an optimal particle size difference for rectifying performance; in most instances, 500-700 samples seem to display the clearest rectifying contact characteristics within the tested range. As the size difference increases beyond this point, forward currents tend to decrease, and the reverse branch region shifts slightly higher, indicating less efficient carrier transport across the junction [7]. Based on the observed curves, the preferred size difference for enhanced rectification appears to be on the order of around 1.25 nm.

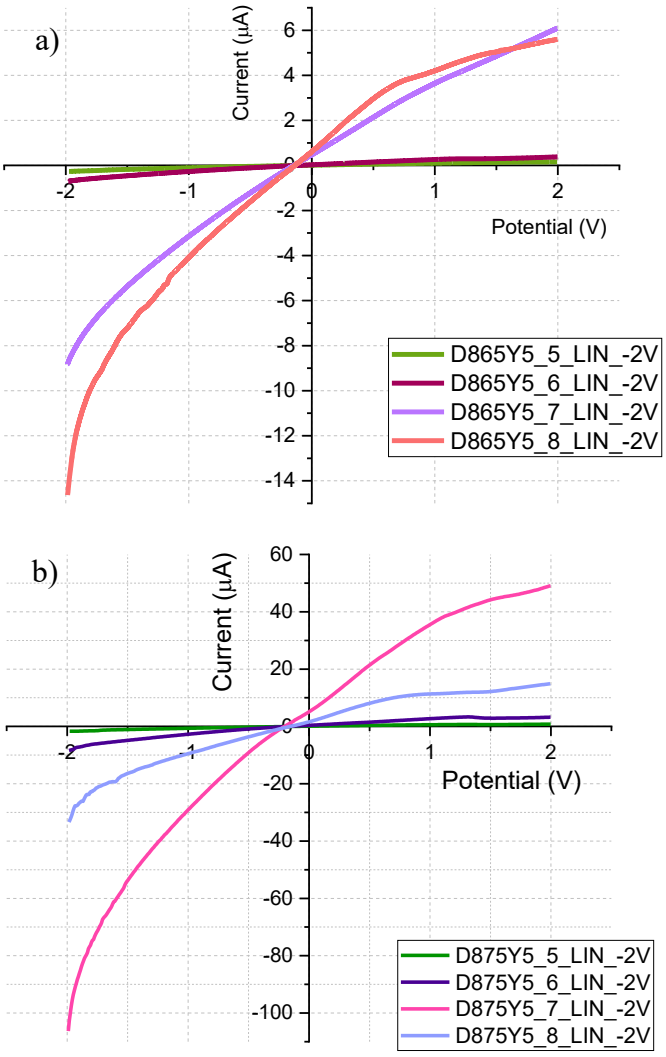

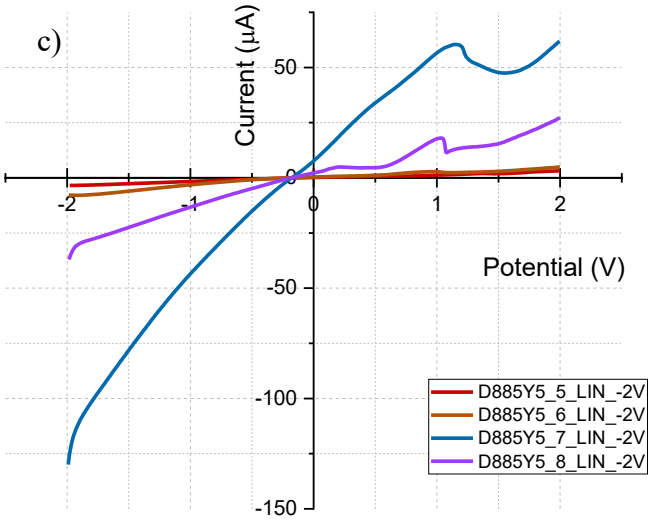

Figure 9. I-V family of curves under deuteration conditions at (a) 65%, (b) 75%, and (c) 85% humidity.

A comparison of the hydration and deuteration measurements shows that the I-V curves' behavior are similar for both processes, with contacts of the same or nearly the same particle size (500-500, 500-600) consistently exhibiting linear, Ohmic-like responses and low current magnitudes, while differently sized contacts (500-700, 500-800) display curvature due to the size gradient between the tested nanoparticle solutions. However, at identical humidity levels, the deuterated samples generally produce higher absolute currents than the hydrated contacts. This is likely because the isotope composition of the moisture source influences the ionic conductivity of the surface layer. Subjected to both hydration and deuteration, the 500-700 contact shows the "best" rectifying contact characteristics at higher humidities, suggesting that there's an ideal size gradient for this application, as previously discussed.

The lack of strong rectifying behavior for most contacts in this study is likely influenced by several factors. The restricted measurement range of ±2 V omits the forward voltage region where Doroshkevich et al. [7] report strong conduction and the characteristic working range of the heterojunction; this can be fixed by extending the measurement ranges up to ±6 V, guaranteeing coverage of strong conducting regions. At the same time, contact pairs with insufficient nanoparticle mismatch, variations in surface and possible non-uniformities in film thickness can all contribute to a more linear response. Finally, polarization effects and ionic accumulation in the hydration layer can shift the I–V curves, further hiding rectifying features in the voltage range.

4. Conclusion

The voltampere characteristics of planar heterojunctions formed by thin films of ZrO_2-8% Y_2O_3 nanoparticles on gold contact pads prepared via drop casting and spray pyrolysis were studied under controlled hydration and deuteration conditions at humidities of 65%, 75%, and 85%. The

reference contact in each pair was fabricated using a 10 nm powder annealed at 500 °C, while the opposing contact was prepared with powders of larger particle size (12–16 nm) obtained through higher annealing temperatures (600–800 °C). Across the measurement range of ±2 V, most contacts exhibited almost linear I-V dependences indicative of Ohmic behavior. Weak rectifying characteristics were observed only in certain pairs, mostly with the 500–700 °C contacts, at the highest humidity levels.

A comparison between hydration and deuteration results showed that similar-sized nanoparticle pairings have comparable tendencies, with 500-700 °C contacts consistently showing the most pronounced curvature. However, deuterated samples generally produced higher currents at the same humidity, suggesting that isotope substitution in the moisture source enhances ionic conduction in the surface layer. Valleys observed in the reverse branches of certain deuterated contacts (500-700 and 500-800) are attributed to dissociation processes within the adsorbed layer.

The absence of strong rectifying behavior in most samples is likely due to a combination of factors; the ±2 V sweep range may only capture a specific part regime of the junction, omitting the working voltage region; variations in morphology and film thickness due to thin-film deposition methods; and polarization of the contact interfaces, which can shift the zero voltage point and hide asymmetry. Extending the voltage range to ±6 V and improving film uniformity through other thin film deposition methods may help to reveal rectifying properties in planar nanoparticle heterojunctions.

5. References

[1] T. Y. Tan and U. Gösele, "Diffusion in Semiconductors," in *Diffusion in Condensed Matter: Methods, Materials, Models*, P. Heitjans and J. Kärger, Eds., Berlin, Heidelberg: Springer, 2005, pp. 165–208. doi: 10.1007/3-540-30970-5_4.

[2] J.-J. Dai *et al.*, "High Hole Concentration and Diffusion Suppression of Heavily Mg-Doped p-GaN for Application in Enhanced-Mode GaN HEMT," *Nanomaterials*, vol. 11, no. 7, Art. no. 7, Jul. 2021, doi: 10.3390/nano11071766.

[3] T. Zhang, C. Hu, and S. Yang, "Ion Migration: A 'Double-Edged Sword' for Halide-Perovskite-Based Electronic Devices," vol. 4, no. 5, 2019, doi: https://doi.org/10.1002/smtd.201900552.

[4] R. Rodriguez, "La teoría de fractales : aplicación experimental e implicaciones en la metodología de la ciencia," Universidad Autónoma de Nuevo León, 1995. [Online]. Available: http://eprints.uanl.mx/377/1/1020114994.PDF

[5] G. Cerofolini, D. Narducci, P. Amato, and E. Romano, "Fractal Nanotechnology," *Nanoscale Research Letters*, vol. 3, pp. 381–385, Jan. 2008, doi: 10.1007/s11671-008-9170-0.

[6] N. Salingaros and A. van Bilsen, *Principles of Urban Structure*. 2005.

[7] A. S. Doroshkevich *et al.*, "The Rectifying Contact of Hydrated Different Size YSZ Nanoparticles for Advanced Electronics," *Nanomaterials (Basel)*, vol. 12, no. 24, p. 4493, Dec. 2022, doi: 10.3390/nano12244493.

[8] B. Oksengendler, S. Maksimov, and V. Nikiforov, "Tamm States of Fractal Surfaces," *Doklady Physics*, vol. 62, pp. 281-283., Jun. 2017, doi: 10.1134/S1028335817060039.

[9] B. Oksengendler and N. Turaeva, “Surface tamm states at curved surfaces of ionic crystals,” *Doklady Physics*, vol. 55, pp. 477–479, Oct. 2010, doi: 10.1134/S1028335810100010.
[10] B. Oksengendler, B. Askarov, I. Nurgaliev, S. Maksimov, and V. Nikiforov, “Nanocatalysis: hypothesis on the action mechanism of gold,” *Nanosystems: Physics, Chemistry, Mathematics*, pp. 249–261, Apr. 2015, doi: 10.17586/2220-8054-2015-6-2-249-261.
[11] M. Kurbanov and B. Oksengendler, “Nanofractals and briquetting technology,” *Journal of Physics: Conference Series*, vol. 2036, p. 012018, Sep. 2021, doi: 10.1088/1742-6596/2036/1/012018.

6. Acknowledgements

The START Program provides an incredible opportunity to gain experience in international teams, laboratories, and research; I’m very grateful towards the START team and fellow participants. Especially, I am grateful to Dr. Aleksandr Doroshkevich for allowing me to join his team, allowing me to learn and gain so much experience. Last but not least, I want to thank Mahmoud Ibrahim for entrusting me with part of his research and knowledge, his patience, and for trusting me to contribute as a colleague, more than a student. I’m looking forward to possible collaborations and I’m eager to return if given the chance.